A Simple Example of Galilean Invariance in the Omega Equation

Michael K. Walters
Department of Engineering Physics, Air Force Institute of Technology, Wright-Patterson AFB, Ohio

ABSTRACT

This paper is pedagogically motivated to qualitatively demonstrate basic concepts related to Galilean invariance and partial cancellation in the individual forcing terms in the traditional form of the omega equation. The analysis provides examples of the vertical distribution of the primary quasigeostrophic (QG) forcing, showing how the individual forcing terms vary in different coordinate systems while their sum remains constant. The QG forcing is described analytically using an unstable Eady wave solution, which allows depictions of QG forcing similar to those in basic atmospheric dynamics texts. The perturbation streamfunction, temperature, and vertical velocity are seen to be invariant under change of horizontal coordinate system, while the individual magnitudes of the QG vertical motion forcing are not. The total QG forcing remains invariant in all cases and is equal to the QG forcing found from the divergence of the **Q** vector. The figures provided can supplement those used for traditional study and may be useful to provoke classroom discussion of related QG concepts.

1. Introduction

The **Q**-vector form of the omega equation (Hoskins et al. 1978) is superior to the traditional, non **Q**-vector form. In **Q**-vector form (assuming $\beta = 0$), there is a single forcing term (related to divergence of **Q**), while the traditional form has two primary forcing terms (differential vorticity advection and the Laplacian of thermal advection), which partially cancel. (Forcing mechanisms involving friction, diabatic heating, and the β effect are not discussed here.) Additionally, the **Q**-vector forcing can be deduced qualitatively from the geopotential and temperature distribution at a single level (unlike the primary forcing in the traditional form), leading to relatively easy interpretation and deduction of regions of strong forcing of quasigeostrophic (QG) vertical motion. The advantages and applications of the **Q**-vector form of the omega equation are well described in the literature, and are not described further here (e.g., Hoskins et al. 1978; Durran and Snellman 1987). Despite the benefits of the **Q**-vector form of the omega equation, students' introduction to quasigeostrophic concepts usually involves the traditional form of the omega equation, which is introduced first in popular atmospheric dynamics textbooks (e.g., Holton 1992 and Bluestein 1992).

Durran and Snellman (1987) and Bluestein (1992) point out that the individual forcing terms in the omega equation are different for identical weather systems that are embedded in mean flows moving at different wind speeds. The individual primary forcing terms differ in each situation because they depend on the motion of the coordinate system in which they are measured, that is, they are not Galilean invariant, although the total primary forcing is Galilean invariant. As Durran and Snellman (1987) and Bluestein (1992) point out, the Galilean variance of the individual primary forcing terms shows that the terms cannot have physical significance in the forcing of vertical motion when considered independently. However, it is difficult for some students to visualize how the primary forcing terms depend on coordinate system, since the Galilean invariance of the total forcing is typically demonstrated only in a mathematical way (e.g., see the derivation in Bluestein 1992, p. 347).

Corresponding author address: Lt. Col. Michael K. Walters, Department of Engineering Physics, Air Force Institute of Technology, 2950 P. Street, Wright-Patterson AFB, OH 45433.
In final form 31 October 2000.

Here, we provide pedagogically motivated figures demonstrating the Galilean invariance and partial cancellation in the individual forcing terms.

The next section briefly reviews QG interpretation of the omega equation, as well as a brief description of the Eady wave solution, which was the basis of the results shown later. The third section presents two specific examples of QG forcing that differ only in that they are embedded in different mean flows; the final section provides conclusions based on these results.

2. Background

a. Forcing of vertical motion in the omega equation

Although the **Q**-vector formulation of the omega equation is superior to the traditional form, students usually begin their study of QG theory with the traditional form of the omega equation. This approach emphasizes a conceptual understanding of the primary forcing mechanisms and the importance of the resulting secondary circulation field in maintaining hydrostatic and geostrophic balance. These physical interpretations are thoroughly discussed by Durran and Snellman (1987), Holton (1992), Bluestein (1992) and others. As a simple example, consider a vertically uniform vorticity field advected by a wind with vertical speed shear and no directional shear, resulting in differential vorticity advection without thermal advection. In this case, positive differential vorticity advection produces increasing cyclonic vorticity with height associated with a decrease in thickness. As a result, there must be a decrease in temperature for the atmosphere to remain hydrostatic. In the absence of horizontal temperature advection, this temperature change is linked to adiabatic cooling associated with an upward secondary circulation. The upward secondary circulations are associated with upper-level divergence and lower-level convergence (due to mass continuity), which produce an opposing change in thermal vorticity. In an analogous way, warm advection, in the absence of differential vorticity advection, is associated with an increase in thickness typically associated with a decrease in the Laplacian of the thickness. Because geostrophic vorticity is proportional to the Laplacian of the geopotential, increasing thickness implies increasingly anticyclonic thermal vorticity for the atmosphere to remain geostrophic. In the absence of vorticity advection, this change in thermal vorticity can be associated with convergence below and divergence above due to upward motion and mass continuity. The upward motion produces adiabatic cooling which offsets the affect of the horizontal warm advection. In each case the secondary circulation opposes the horizontal advection and acts to restore the atmosphere to hydrostatic and geostrophic balance, which is an example of LeChatelier's principle (Bluestein 1992). While these two examples are useful, interpreting the terms individually avoids the cancellation in the individual forcing terms in the omega equation discussed below. The concepts described here also disregard the fact that the primary forcing terms do not really have physical significance because they are not Galilean invariant. The use of the word "forcing" to describe these terms in unfortunate, as it is just as accurate to say that the vertical motion "forces" the differential vorticity advection and horizontal temperature advection, or that the differential vorticity advection forces both the vertical motion and the horizontal temperature advection. It must be emphasized that there is not a cause and effect relationship between the primary forcing terms and QG vertical motion, since each occurs simultaneously.

A similar physical interpretation can also be made for the forcing in the **Q**-vector form of the omega equation. The derivation of the **Q** vector mathematically demonstrates that horizontal geostrophic advection breaks down the thermal wind balance in the absence of compensating ageostrophic motions, which are required to maintain hydrostatic and geostrophic balance. The **Q** vector itself is proportional to the rate of change of the horizontal temperature gradient following geostrophic advection. Therefore, convergence of the **Q** vector implies a local increase in thickness. For the atmosphere to remain hydrostatic and geostrophic, there must be an increase in anticyclonic thermal vorticity (an upward motion according to the vorticity equation) or a compensating decrease in temperature from other mechanisms (such as upward motion and adiabatic cooling through the thermodynamic equation). As a result, a geostrophic disturbance is accompanied by both horizontal adjustments in the temperature field as a result of spatially varying vertical motions, and adjustments in the vertical wind field due to vertical variations in the ageostrophic wind. The resulting temperature changes (from the vertical motion) and the parcel accelerations (due to the ageostrophic wind) both act to offset the disruption in thermal wind balance and act to restore the hydrostatic and geostrophic balance (Durran and Snellman 1987; Holton 1992; Bluestein 1992).

Studying the physical interpretation of the primary forcing terms in the traditional form of the omega equation involves assessing their sign at strategic locations in the midlevel geopotential field while neglecting the cancellation between the terms (i.e., the terms are considered individually). Such exercises are often based on simplified schematic synoptic conditions, which show the tilt with height of perturbation geopotential and perturbation temperature that are characteristic of a developing baroclinic wave (e.g., see Fig. 6.6 in Holton 1992). Also, the assumption is usually made that the left-hand side of the omega equation is proportional to $-\omega$ due to the elliptic form of the operator. These exercises are useful to learn about the mathematical and physical nature of the omega equation and to introduce the role of the secondary circulation in maintaining hydrostatic and geostrophic balance described above. However, students may be frustrated in attempts at deciphering the signs of the primary forcing terms at locations in the wave where cancellation between the terms makes the situation more problematic. This frustration is not alleviated when students subsequently learn that the forcing terms are not really physically meaningful due to a coordinate-dependent partial cancellation between the two forcing terms.

b. The Eady solution

The Eady wave (Eady 1949) provides a conceptually simple and elegant model of baroclinic instability. In particular, the unstable Eady wave solution shows the westward tilt with height of perturbation geopotential and eastward tilt with height of the perturbation temperature that is characteristic of a developing baroclinic wave. The Eady model successfully predicts the characteristic wavelength and growth rate of midlatitude transient disturbances, as well as a poleward temperature flux consistent with energetic explanations of baroclinic instability (Pedlosky 1987; Holton 1992; James 1994). The relationship between the geopotential and temperature is similar to that in the simple baroclinic waves used to study QG theory. Because the Eady solution can be described analytically for a given constant thermal wind, it is relatively straightforward to calculate the QG forcing in the omega equation by assuming the horizontal wind in the Eady solution is geostrophically balanced.

The Eady wave solution is derived for a fluid that is situated between two rigid surfaces on an f plane, so the β effect is not included. The meridional temperature gradient (and therefore thermal wind) is assumed to be constant. A drawback of the Eady solution is that it does not allow for meridional tilt of the unstable waves, which is unrealistic because it does not allow for meridional momentum flux [which is also true for the Charney (1947) baroclinic instability model, which is somewhat more complicated]. Because the Eady model is capped by a rigid lid, it predicts an upper-level boundary wave, which is not realistic in the atmosphere. The presence of the rigid upper lid is necessary for baroclinic instability to occur in the Eady model because the potential vorticity gradient in the interior is zero (Pedlosky 1987). Despite the fact that the Eady wave is unrealistic in comparison to the actual atmosphere in some respects, the Eady solution is mathematically consistent with the linearized quasigeostrophic momentum and thermodynamic equation. Therefore, the Eady solution provides a valid example of Galilean invariance in the omega equation described previously. Finally, because there is some dynamic similarity between a rigid upper lid and the tropopause (Morgan and Nielson-Gammon 1998), it can be argued that the distribution of variables beneath the rigid lid should be analogous to the distribution of variables beneath the tropopause in the real atmosphere.

c. Procedure

The Eady wave solution used here is a slight modification of that derived in James (1994), which is based on a basic state with equal and opposite zonal winds at the top and bottom boundary. Here, the basic-state streamfunction is modified to allow the addition of a constant zonal wind at all levels (defined as the constant c). The influence of this modification on the Eady wave derivation is described in the appendix.

A constant thermal wind of U/H is assumed, where U is the difference in zonal wind from top to bottom, which are at $z^* = \pm H/2$ where H is the depth. Two separate cases are considered—one with $c = 0$, which is the same as the solution in James (1994), and one with $c = U/2$, where the wind at the bottom is 0 and the zonal wind at the top is U. In each case the thermal wind is the same, and the resulting Eady solutions are identical (except for the difference in phase; they are identical when the abscissa is $x + ct$).

There are two forms of the omega equation of interest here. Details of the derivation and the definition of the symbols are provided in the appendix. The first form of the omega equation is the standard form (in log-pressure coordinates),

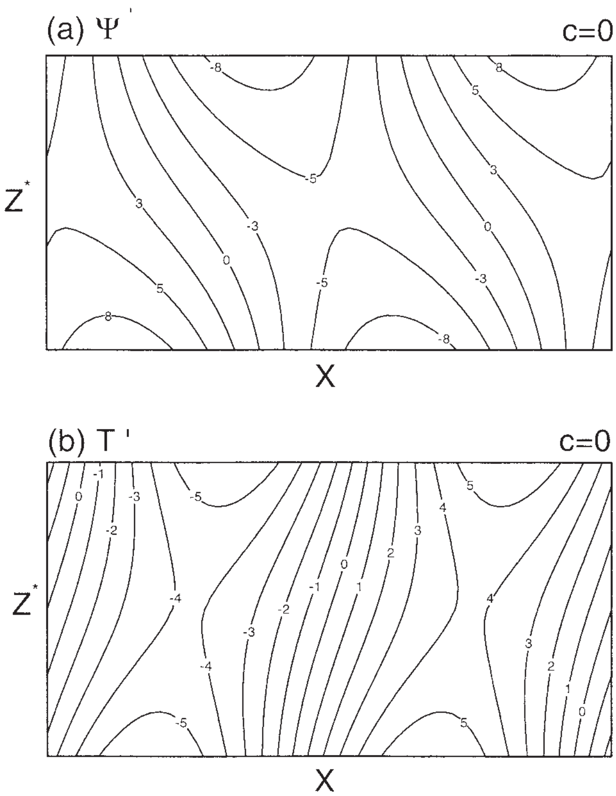

FIG. 1. (a) Cross section of perturbation streamfunction Ψ' ($\times 10^{-6}$ m^{2}s^{-1}) for $c = 0$ case. (b) Cross section of perturbation temperature T' (K) for $c = 0$ case.

$$N^2\nabla^2 w^* + f_0^2 \frac{\partial}{\partial z^*}\left(\frac{\partial w^*}{\partial z^*} - \frac{w^*}{H}\right) = \Omega 1 + \Omega 2, \quad (1)$$

where $w^* = dz^*/dt$ is the vertical velocity. The primary forcing term Ω1 represents differential vorticity advection, while Ω2 represents the Laplacian of the thickness advection in the following discussion. These primary forcing terms are described in the appendix. The vertical motion field described by Eq. (1) is due to the sum Ω1 + Ω2, and there is no time derivative in the equation, which is therefore diagnostic for w^*. As described previously and shown in the appendix, Ω1 and Ω2 can be rearranged to show that they each include a common factor, which cancels between them. As a result, for a given thermal wind, there is an infinite number of Eady solutions (each with a different c) that produces the same (phase shifted) QG vertical motion field. In each case, the distributions of Ω1 and Ω2 will be different, while the total forcing Ω1 + Ω2 is identical (although phase shifted).

The second form of the omega equation of interest (briefly discussed in the appendix) is the equivalent **Q**-vector form

$$N^2\nabla^2 w^* + f_0^2 \frac{\partial}{\partial z^*}\left(\frac{\partial w^*}{\partial z^*} - \frac{w^*}{H}\right) = 2\nabla\cdot\mathbf{Q}. \quad (2)$$

The right-hand side of Eq. (2) is positive in this derivation, as convergence of **Q** is associated with upward vertical motion ($w^* > 0$) if the left side of the equation is proportional to $-w^*$. Because the total forcing determined from the divergence of **Q** is identical to Ω1 + Ω2 (shown in the appendix), the **Q**-vector form of the omega equation is not discussed further here.

The Eady wave parameters are chosen so that the resulting perturbation has complex frequency and is therefore unstable. Specifying the frequency also determines the vertical tilt of the geopotential and temperature perturbations. From the resulting form of perturbation streamfunction ψ' and the basic-state streamfunction ψ, the various quantities on the right-hand side of Eqs. (1) and (2) can be calculated using their analytical forms given in the appendix. The results are consistent, in that Ω1 + Ω2 and $2\nabla \cdot \mathbf{Q}$ are equivalent. In addition, the advection of relative vorticity by the thermal wind (following the approximation in Trenberth 1978) is also proportional to the total

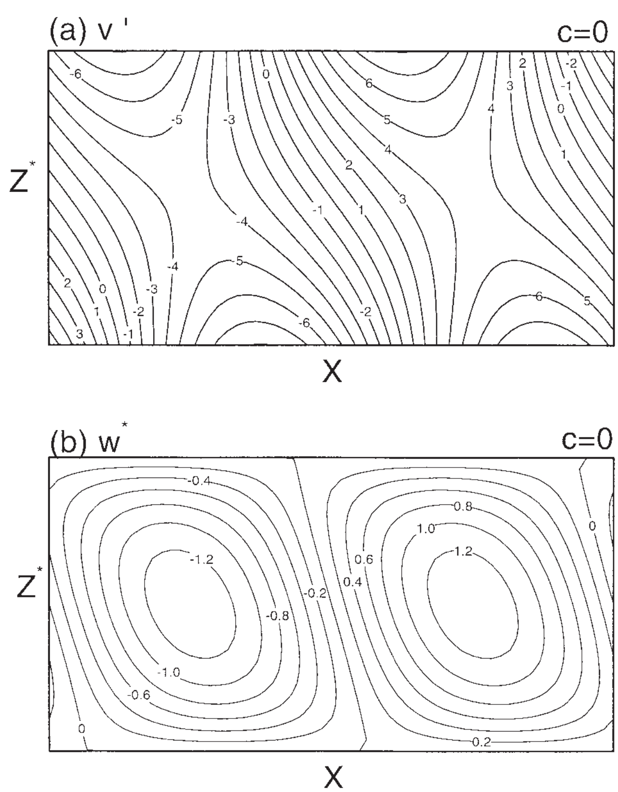

FIG. 2. (a) Cross-section meridional velocity v' (m s^{-1}) for c = 0 case. (b) Cross section of vertical velocity w^* (cm s^{-1}) for c = 0.

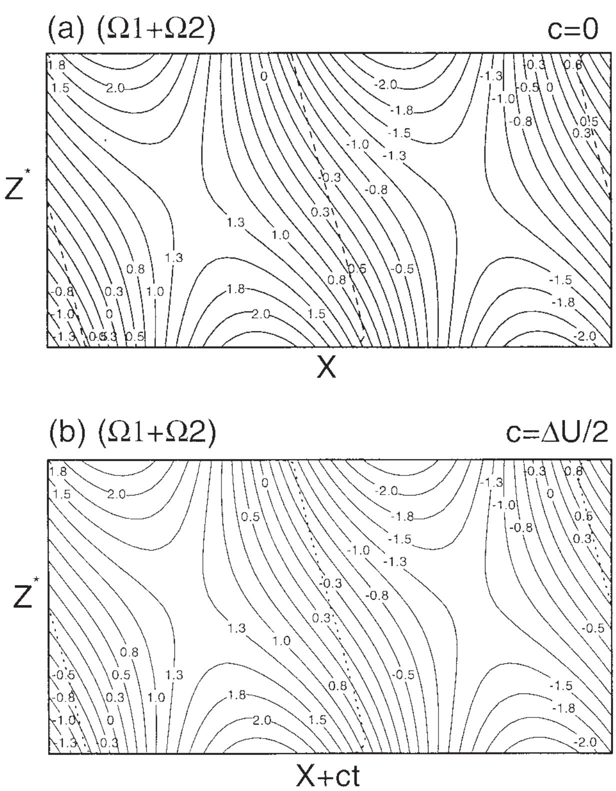

FIG. 3. (a) Cross section of the total primary forcing $\Omega 1 + \Omega 2$ ($\times 10^{17}$ (m^{-1} s^{-3}) for $c = 0$. (b) As in (a) but for $c = \Delta U/2$.

primary forcing and is invariant to changes in constant zonal wind because it is not a function of c. This result is also consistent with the derivation presented in Bluestein (1992), since the derivation here is carried out for constant f and the deformation of the horizontal wind is identically zero (not shown here). The individual terms $\Omega 1$ and $\Omega 2$ are each functions of c, so they are not Galilean invariant as described above.

3. Results

A few selected results are shown for each case described above to describe the Galilean invariance of the total primary forcing and the Galilean variance of the individual terms. The first case ($c = 0$) results in a zonal wind, which is zero at the ground and U at the top of the model, while the second case ($c = \Delta U/2$) results in an antisymmetric zonal wind about the midlevel. The perturbation Eady wave structure of each case is identical, provided the horizontal coordinate in the plots is $x + ct$.

Figures 1a and 1b show vertical cross sections at $y = 0$ of perturbation streamfunction ψ' and temperature T'. The results shown are for the $c = 0$ case; the results for the $c = \Delta U/2$ case are identical after accounting for the phase difference. These figures show the westward slope with height of perturbation streamfunction and eastward slope with height of perturbation temperature that is characteristic of developing baroclinic waves. This vertical structure is very similar to schematic models often used to introduce QG concepts. Figures 2a and 2b show the corresponding vertical cross sections of the meridional velocity v' and the vertical velocity w^*.

Figures 3a and 3b show vertical cross sections of $\Omega 1 + \Omega 2$ for each case. Also shown in each figure (dashed) is the $w^* = 0$ contour from Fig. 2b to delineate the two regions of vertical motion. The common assumption that the left side of Eq. (1) is proportional to $-w^*$ can be checked by comparing the sign of $\Omega 1 + \Omega 2$ with the sign of the vertical velocity from Fig. 2b. For example, if the assumption is valid, regions of $\Omega 1 + \Omega 2 < 0$ will correspond to upward vertical motion, $w^* > 0$. These examples show that the assumption holds over most of the domain, except for small areas near the $w^* = 0$ contour. These figures

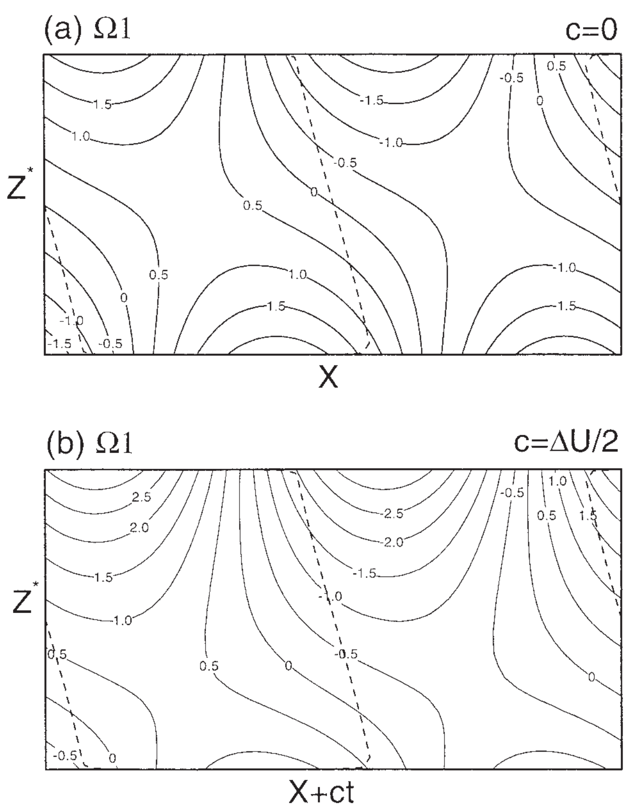

FIG. 4. (a) Cross section of the primary forcing $\Omega 1$ ($\times 10^{17}$ m^{-1} s^{-3}) for $c = 0$. The dash–dot contour in each figure is $w^* = 0$. (b) As in (a) but for $c = \Delta U/2$.

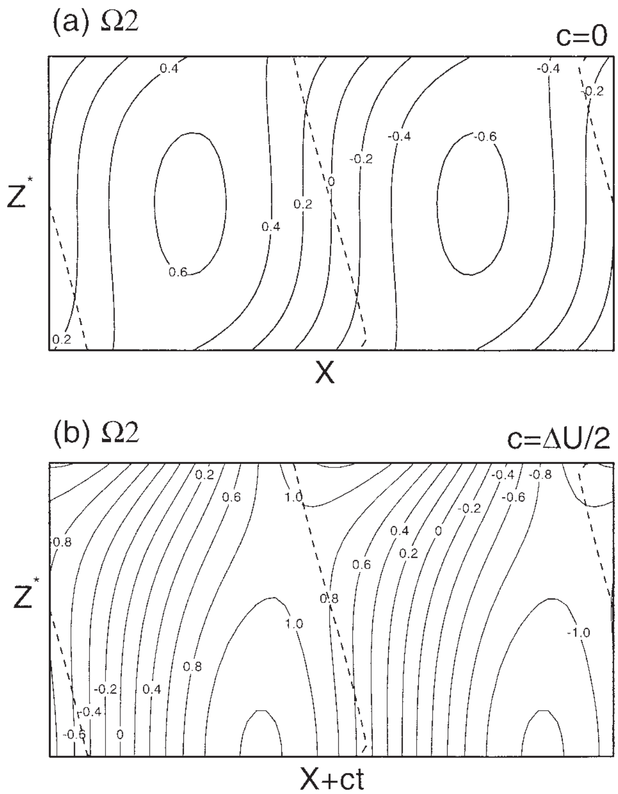

FIG. 5. (a) Cross section of the primary forcing Ω2 ($\times 10^{17}$ m^{-1}s^{-3}) for $c = 0$. The dash–dot contour in each figure is $w^* = 0$. (b) As in (a) but for $c = \Delta U/2$.

show that the total forcing Ω1 + Ω2 is invariant to changes in c.

Vertical cross sections of the individual primary forcing terms are shown in Figs. 4a and 4b (Ω1) and Figs. 5a and 5b. (Ω2) for each case with the dashed $w^* = 0$ contour (from Fig. 2b). These figures show areas where the sign of each of the individual primary forcing terms is not proportional to $-w^*$; these areas are different in each case. As described above, Ω1 < 0 would be associated with $w^* > 0$, if we assume the left-hand side of Eq. (1) is proportional to $-w^*$ (and neglect the contribution of Ω2). Using this assumption, it may not be accurate to use Ω1 (or Ω2) by itself to diagnose QG vertical motion in regions where Ω1 (or Ω2) and w^* are the same sign. Figures 4 and 5 show that the individual primary forcing terms vary between cases (they are not Galilean invariant).

Figures 6a and 6b shows contours of the term that cancels between the primary forcing terms Ω1 and Ω2 (described in the appendix). The region of cancellation is different in each case. Finally, the horizontal relative QG vorticity advection, $\mathbf{V}_g \cdot \nabla\zeta_g$, shown in Figs. 7a and 7b, is considerably different between cases. In the $c = 0$ case, the basic state wind is antisymmetric about the midlevel ($z^* = 0$) and the maximum vertical velocity occurs at a level where the horizontal vorticity advection is zero. While this is a contrived example, this result emphasizes that the mechanism of interest in the diagnosis of QG vertical motion is differential vorticity advection and not horizontal vorticity advection at a particular level.

Since the total primary omega equation forcing is invariant to changes in coordinate system, we are free to choose any such moving coordinate system to describe the total forcing. As shown in the appendix, the partial cancellation between the primary forcing terms vanishes when $z^* = -cH/U$. This occurs for $c = 0$ at the level $z^* = 0$ (exactly at midlevel) as shown in Fig. 6a. Therefore, for $c = 0$, the individual primary forcing terms in the omega equation can be interpreted at the midlevel ($z^* = 0$) in a way that describes well LeChatelier's principle as applied to the maintenance of hydrostatic and geostrophic balance via secondary circulations. As a result, the total forcing terms at midlevels for $c = 0$ conform well to the concepts described in section 2 and the interpretation of vertical

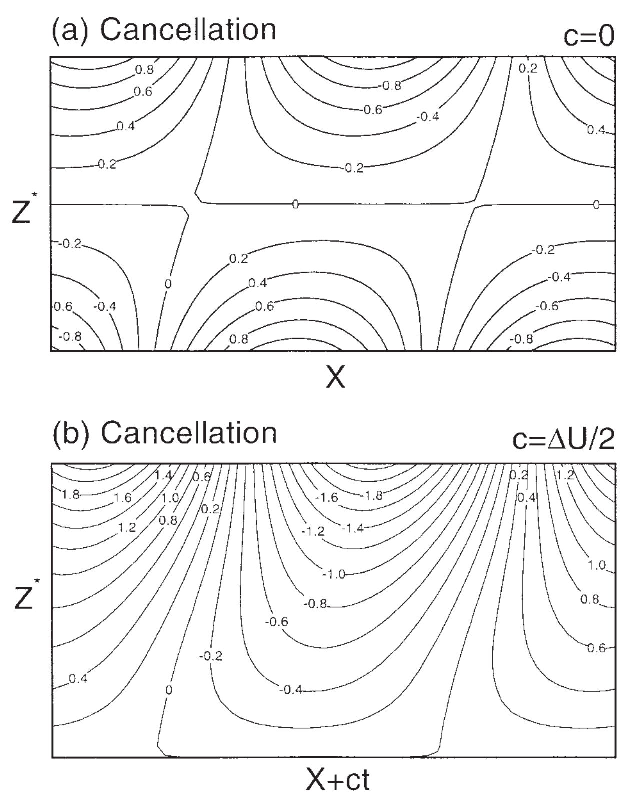

FIG. 6. (a) Cross section of the cancellation [given by (A16)] between Ω1 and Ω2 ($\times 10^{17}$ m^{-1}s^{-3}) for $c = 0$. (b) As in (a) but for $c = \Delta U/2$.

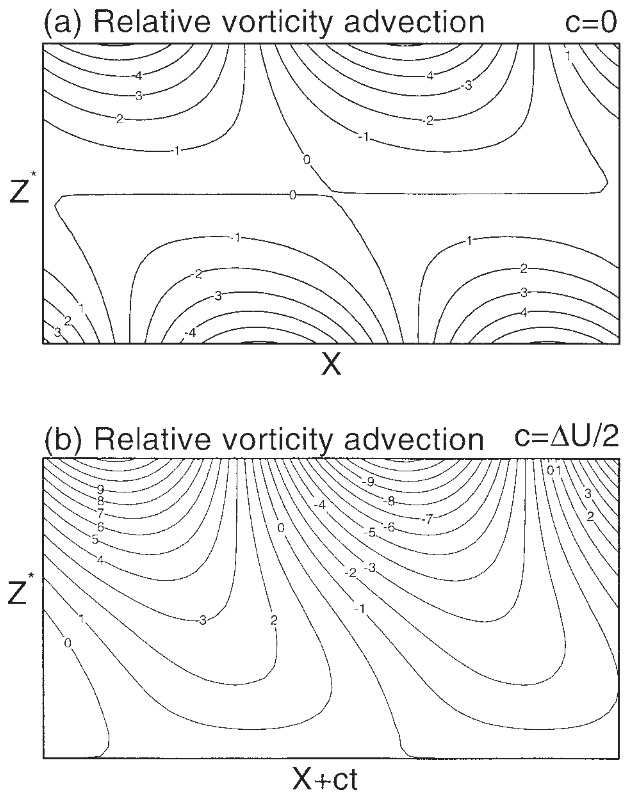

FIG. 7. (a) Horizontal geostrophic vorticity advection, $\mathbf{V}_g \cdot \nabla\zeta_g$ ($\times 10^{10}\mathrm{s}^{-2}$), for $c = 0$. (b) As in previous figure but for $c = \Delta U/2$.

motion using either of the primary forcing terms is qualitatively the same as using the total primary forcing.

Because the schematic wave used here is simple (consisting of a single wavenumber horizontally), a caveat is appropriate. The assumption that the left-hand side of the omega equation is proportional to $-w^*$ is very accurate here as shown above, so the correspondence between the individual forcing terms and the vertical motion is also very good. In reality, there may be significant areas at midlevels where this assumption is not accurate (see Durran and Snellman 1987 for a good example). As a result, the estimation of vertical motion from the total primary forcing in such areas may be less useful (even using the **Q**-vector formulation).

4. Conclusions

The figures shown provide graphical examples of the Galilean variance of the primary forcing terms in the omega equation and the resulting variation in the distribution of QG forcing of vertical motion. The following points can be summarized.

- Because Ω1 and Ω2 are not invariant in two identical systems embedded in mean flows moving at different wind speeds, there are regions where either term (considered by itself) may not be a good indication of vertical motion. These regions may vary considerably between cases.
- Because Ω1 + Ω2 is invariant, the region where the total primary forcing accurately predicts vertical motion (assuming that the left side of the omega equation is the negative of vertical velocity) is always the same. For the wave structure chosen here, this region is quite large, which indicates that the vertical motion determined by the **Q** vector at midlevels would be quite accurate in this example.
- There may be regions of the wave at midlevels where individual interpretation of the primary forcing mechanisms is less helpful in diagnosis of the sign of vertical motion, as in the case where $c = \Delta U/2$.
- These results reemphasize that the **Q**-vector form of the omega equation is preferable.
- The general rule that cyclonic vorticity advection (anticyclonic vorticity advection) aloft is indicative of vorticity advection increasing (decreasing) with height and upward (downward) motion is generally accurate in the $c = U/2$ case, but misleading in the $c = 0$ case if applied at or below the level where the horizontal vorticity advection is zero (which is the level of maximum vertical velocity).

Acknowledgments. The author acknowledges the helpful comments of Dr. John Nielson-Gammon, which greatly improved the manuscript. The views expressed in this article are those of the author and do not reflect the official policy or position of the United States Air Force, Department of Defense, or the U.S. government.

Appendix: Mathematical details

The QG omega equation in log-pressure coordinates follows directly from the frictionless QG momentum equations on the f plane where $f = f_0$:

$$\frac{\partial u_g}{\partial t} + u_g \frac{\partial u_g}{\partial x} + v_g \frac{\partial u_g}{\partial y} - f_0 v_a = 0 \qquad \text{(A1)}$$

$$\frac{\partial v_g}{\partial t} + u_g \frac{\partial v_g}{\partial x} + v_g \frac{\partial v_g}{\partial y} + f_0 u_a = 0. \qquad \text{(A2)}$$

In Eqs. (A1) and (A2) the subscript g refers to the geostrophic wind and the subscript a refers to the ageostrophic wind. The adiabatic thermodynamic equation is

$$\left(\frac{\partial}{\partial t}+u_g\frac{\partial}{\partial x}+v_g\frac{\partial}{\partial y}\right)\frac{\partial\Phi}{\partial z^*}+w^*N^2=0, \quad \text{(A3)}$$

where Φ is the geopotential and N is the Brunt–Väisälä frequency. The vertical log-pressure coordinate is defined by

$$z^*=-H\ln\left(\frac{p}{p_0}\right). \quad \text{(A4)}$$

Following the general procedure (e.g., see Holton 1992, 170–173 Bluestein 1992, 350–353), the QG omega equation can be found to be

$$N^2\nabla^2w^*+f_0^2\frac{\partial}{\partial z^*}\left(\frac{\partial w^*}{\partial z^*}-\frac{w^*}{H}\right)=\Omega1+\Omega2, \quad \text{(A5)}$$

where the forcing terms are

$$\Omega1=f_0\frac{\partial}{\partial z^*}\left(u_g\frac{\partial}{\partial x}+v_g\frac{\partial}{\partial y}\right)\left(\frac{1}{f_0}\nabla^2\Phi\right), \quad \text{(A6)}$$

which represents differential vorticity advection, and

$$\Omega2=-\nabla^2\left(u_g\frac{\partial}{\partial x}+v_g\frac{\partial}{\partial y}\right)\left(\frac{\partial\Phi}{\partial z^*}\right),$$

which is the Laplacian of the thickness advection.

Following the basic derivation in Holton (1992), the **Q**-vector form of the QG omega equation follows from the momentum, thermodynamic, and continuity equations and is given by

$$N^2\nabla^2w^*+f_0^2\frac{\partial}{\partial z^*}\left(\frac{\partial w^*}{\partial z^*}-\frac{w^*}{H}\right)=2\nabla\cdot\mathbf{Q}, \quad \text{(A7)}$$

where the components of the **Q** vector are given by

$$Q_1=-\left[\frac{\partial u_g}{\partial x}\frac{\partial}{\partial x}\left(\frac{\partial\Phi}{\partial z^*}\right)+\frac{\partial v_g}{\partial x}\frac{\partial}{\partial y}\left(\frac{\partial\Phi}{\partial z^*}\right)\right] \quad \text{(A8)}$$

$$Q_2=-\left[\frac{\partial u_g}{\partial y}\frac{\partial}{\partial x}\left(\frac{\partial\Phi}{\partial z^*}\right)+\frac{\partial v_g}{\partial y}\frac{\partial}{\partial y}\left(\frac{\partial\Phi}{\partial z^*}\right)\right]. \quad \text{(A9)}$$

The right-hand side of Eq. (A7) is positive, so that convergence of **Q** gives upward vertical motion as in the typical definition in p coordinates. Equations (A8) and (A9) are analogous to the definition in Holton.

The derivation of the Eady solution (Eady 1949) used here follows the derivation in James (1994), which assumes a vertically symmetric basic state in log-pressure coordinates, with the top of the domain at $z^* = H/2$ and the bottom at $z^* = -H/2$. The basic-state streamfunction ψ is a slight modification of the form given in James (1994) and is given by

$$\Psi=-\frac{Uyz^*}{H}-cy+F, \quad \text{(A10)}$$

where c represents a constant zonal wind throughout the depth of the model (H) and ψ is related to geopotential of the f plane by $f_0\psi = \Phi$, and F represents an additive constant. In Eq. (A10), U/H represents the constant thermal wind. Because the additive constant F is not a function of x and y, it does not appear in the following derivation and does not need to be considered further.

The term c was added to make it easy to show the invariance of the QG forcing to the addition of a constant zonal wind. With $c = 0$ the Eady solution follows the same as in James (1994, 138–141). We assume a solution for the perturbation streamfunction Ψ':

$$\psi' = \phi(z^*)\cos(ly)\exp[i(kx - wt)],$$

where k and l are horizontal wavenumbers in x and y. Conservation of potential vorticity leads to an ordinary differential equation for the perturbation streamfunction amplitude $\phi(z^*)$ whose solution is

$$\phi(z^*) = [A\cosh(z/H_r) + B\sinh(z/H_r)],$$

where A and B are constants that can be determined from the boundary conditions $w^* = 0$ at the top and bottom of the model. The resulting dispersion equation for the Eady solution including the phase shift c is given by

$$\omega = kc \pm kU\sqrt{\left[\frac{1}{2}\tanh\left(\frac{K}{2K_r}\right)-\frac{K_r}{K}\right]\left[\frac{1}{2}\coth\left(\frac{K}{2K_r}\right)-\frac{K_r}{K}\right]}, \quad \text{(A11)}$$

where $K = \sqrt{k^2 + l^2}$ represents the total wavenumber and $K_r = f/(NH)$. This result is the same as the result in James (1994) with the addition of the constant basic state frequency kc. For complex ω, the solution is unstable. For the Eady solutions plotted here, $k = l$, which results in a square wave in the horizontal, and $K = 1.61K_r$, which is the total wavenumber of the solution with the fastest growth rate for $l = 0$ (James 1994). This choice of K does not result in the fastest growing wave for the square wave used here, but the result is representative of an unstable baroclinic wave.

By assuming appropriate values for ω and assuming that the total horizontal wind in the Eady solution is in geostrophic balance, we can find the various forcing terms, which appear in the omega equation. These include the relative vorticity

$$\zeta = -\cos(ly)\exp[i(kx - wt)](k^2 + l^2)\phi(z^*), \qquad \text{(A12)}$$

the relative vorticity advection

$$u\frac{\partial \zeta}{\partial x} + v\frac{\partial \zeta}{\partial y} = -i\phi\cos(ly)k\exp[i(kx - wt)] \times (k^2 + l^2)\frac{Uz^* + cH}{H}, \qquad \text{(A13)}$$

the differential vorticity advection

$$\Omega 1 = -if_0\cos(ly)k\exp[i(kx - wt)](k^2 + l^2) \times \left[\frac{UH_rAC + UH_rBS + (Uz^* + cH)(AS + BC)}{H_rH}\right], \qquad \text{(A14)}$$

and the Laplacian of the thickness advection

$$\Omega 2 = if_0\cos(ly)k\exp[i(kx - wt)](k^2 + l^2) \times \left[\frac{(Uz^* + cH)(AS + BC) - UH_rAC - UH_rBS}{HH_r}\right], \qquad \text{(A15)}$$

where $S = \sinh(K/2K_r)$, $C = \cosh(K/2K_r)$ following the notation in James (1994). Equations (A14) and (A15) show that each of the individual forcing terms in the traditional form of the omega equation vary by the addition of a constant zonal wind (c). The common expression that cancels between the terms is

$$-if_0\cos(ly)k\exp[i(kx - \omega t)] \times (k^2 + l^2)\left[\frac{(Uz^* + cH)(AS + BC)}{HH_r}\right]. \qquad \text{(A16)}$$

This expression is related to the advection of thermal vorticity by the constant zonal wind, since

$$c\frac{\partial}{\partial x}\left(\frac{\partial}{\partial z}\nabla^2\Phi\right) = -icf_0\cos(ly)k\exp[i(kx - \omega t)] \times (k^2 + l^2)\left[\frac{AS + BC}{H_r}\right].$$

The factor $Uz^* + cH$ vanishes when $c = -Uz^*/H$ or $z^* = -cH/U$, which is the level where $\Psi = 0$ by Eq. (A10). Therefore, at $z^* = 0$ and $c = 0$, the cancellation between the terms is zero. The existence of this term shows that the individual terms are not invariant to changes in c.

The total forcing of the ω equation in the form of Eq. (A5) is given by

$$\Omega 1 + \Omega 2 = -2if_0\cos(ly)k\exp[i(kx - \omega t)] \times (k^2 + l^2)\frac{U}{H}\phi. \qquad \text{(A17)}$$

This result shows that the total forcing is invariant to the additional of a constant zonal wind as expected and is linear with respect to the thermal wind U/H. Similarly, the components of the **Q** vector can be found to be

$$Q1 = -\phi k^2 f_0\cos(ly)\exp[i(kx - \omega t)]\frac{U}{H} \qquad \text{(A18)}$$

and

$$Q2 = -i\phi l\exp[i(kx - \omega t)] \times kf_0\left[\frac{l\exp[i(kx - \omega t)](HAS + HBC) + \sin(ly)UH_r}{HH_r}\right],$$

from which

$$2\nabla \cdot \mathbf{Q} = -2if_0\cos(ly)k\exp[i(kx - \omega t)] \qquad \text{(A19)}$$

$$\times (k^2 + l^2)\frac{U}{H}\phi = \Omega 1 + \Omega 2, \qquad \text{(A20)}$$

which is identical to the previous result in Eq. (A17).

It is interesting to note that the advection of vorticity by the thermal wind is given by

$$\frac{\partial \mathbf{V}_g}{\partial z} \cdot \nabla \zeta = -i \cos(ly) k \exp[i(kx - \omega t)] \times (k^2 + l^2) \frac{U}{H} \phi = \frac{1}{2 f_0} (\Omega 1 + \Omega 2), \tag{A21}$$

which is Trenberth's approximation (Trenberth 1978). Another interesting feature of this solution is that

$$\frac{\Omega 1 + \Omega 2}{v} = -2(k^2 + l^2) U \frac{f}{H}, \tag{A22}$$

so that the perturbation meridional velocity is proportional to the negative of the total omega forcing for this choice of Ψ. This relationship can be seen clearly in the figures.

References

Bluestein, H. B., 1992: *Principles of Kinematics and Dynamics.* Vol. 1. *Synoptic-Dynamic Meteorology in Midlatitudes*, Oxford University Press, 448 pp.

Charney, J. G., 1947: The dynamics of long waves in a baroclinic westerly current. *J. Meteor.,* **4,** 135–163.

Durran, D. R., and L. W. Snellman, 1987: The diagnosis of synoptic-scale vertical motion in an operational environment. *Wea. Forecasting,* **2,** 17–31.

Eady, E. T., 1949: Long waves and cyclone waves. *Tellus,* **1** (3), 33–52.

Holton, J. R., 1992: *An Introduction to Dynamic Meteorology.* Academic Press, 507 pp.

Hoskins, B. J., I. Draghici, and H. C. Davies, 1978: A new look at the ω-equation. *Quart. J. Roy. Meteor. Soc.,* **104,** 31–38.

James, I., 1994: *Introduction to Circulating Atmospheres.* Cambridge University Press, 422 pp.

Morgan, M. C., and J. W. Nielson-Gammon, 1998: Using tropopause maps to diagnose midlatitude weather systems. *Mon. Wea. Rev.,* **126,** 2555–2579.

Pedlosky, J., 1987: *Geophysical Fluid Dynamics.* Springer-Verlag, 710 pp.

Trenberth, K. E., 1978: On the interpretation of the diagnostic QG omega equation. *Mon. Wea. Rev.,* **106,** 131–137.